Landslides
DOI 10.1007/s10346-019-01287-4
Received: 12 March 2019
Accepted: 13 September 2019

Gordon G. D. Zhou · Junhan Du · Dongri Song · Clarence E. Choi · H. S. Hu · Chenghua Jiang

Numerical study of granular debris flow run-up against slit dams by discrete element method

Abstract Run-up of granular debris flows against slit dams on slopes is a complex process that involves deceleration, deposition, and discharge. It is imperative to understand the run-up mechanism and to predict the maximum run-up height for the engineering design and hazard mitigation. However, the interaction between granular flows and slit dams, which significantly affects the run-up height, is still not well understood. In this study, an analytical model based on the momentum approach was derived to predict the run-up heights of granular debris flows. A numerical investigation of granular debris flow impacting slit dams using the discrete element method (DEM) was then conducted. The influence of the Froude number (N_{Fr}) and the relative post spacing (R) on run-up height were studied. This study illustrates that the analytical model based on the momentum approach can predict the run-up heights well within a certain range of Froude numbers. There is a critical value of relative post spacing (R_C): within the critical value, the maximum run-up height is insensitive to the relative post spacing; once R exceeds the critical value, the maximum run-up height decreases rapidly as the relative post spacing increases.

Keywords Granular debris flow · Slit dam · Soil/structure interaction · Run-up height

Introduction

Granular debris flows comprise a wide range of particle sizes (Jakob et al. 2005), surging down slopes in response to gravity (Iverson 1997). Due to the high mobility and the large volume of material (Shen et al. 2018), granular debris flows can result in disastrous consequences to human lives and facilities downstream (Hungr et al. 1984).

To mitigate such destructive hazards, slit structures such as slit dams (Watanabe et al. 1980; Armanini et al. 2011; Piton and Recking 2015a; Marchelli et al. 2019; Zhou et al. 2019) and baffle arrays (Choi et al. 2014a Law et al. 2015) are often strategically installed along the predicted flow path. Such structures, comprising rigid planes (hereafter referred to as "posts") and openings (referred to throughout as "slits"), can dissipate flow energy, thereby arresting flows (Choi et al. 2014a Zhou et al. 2019).

Granular debris flows impact rigid barriers and transfers momentum vertically into run-up, potentially overtopping obstacles (Hákonardóttir 2003 Ng et al. 2016). Design of engineering countermeasures requires estimates of run-up height to prevent overtopping (Kwan 2012 Choi et al. 2016 Ng et al. 2017). However, existing physically based debris flow models may be unable to output the maximum run-up heights accurately (Choi et al. 2015b Iverson et al. 2016), given the complexity of the problem.

Multiple analytical models have been proposed to predict the maximum run-up heights of granular avalanches/flows against rigid barriers (Hungr and McClung 1987 Chu et al. 1995 Mancarella and Hungr 2010). Nevertheless, there are two commonly adopted approaches for predicting debris flow run-up height in practice (Kwan 2012)—the energy approach (Armanini et al. 2011 Kwan 2012) and the momentum approach proposed by Hákonardóttir (2003) and Jóhannesson et al. (2009). The energy approach (Armanini et al. 2011 Kwan 2012) is given as follows:

$$\frac{h_f}{h_i} = 1 + \frac{u^2}{2gh_i} \tag{1}$$

where h_f is the run-up height, h_i is the height of incoming flow, u is the incoming flow velocity, and g is the acceleration due to gravity.

Another commonly adopted approach proposed by Jóhannesson et al. (2009) is based on conservation of mass and momentum:

$$\frac{\rho_f}{\rho_i}\left(\frac{h_f}{h_i}\right)^2 - \frac{h_f}{h_i} + \left(\frac{\rho_f h_f}{\rho_i h_i}\right)^{-1} - 1 - 2N_{Fr}^2 = 0 \tag{2}$$

where ρ_f is the density of the flow after run-up and ρ_i is the density of the incoming flow. N_{Fr} is the Froude number of the incoming flow, indicating the ratio of inertial forces to gravitational forces. Subcritical and supercritical flow conditions are characterized with Froude numbers less than and greater than unity, respectively (Choi et al. 2015a; Ng et al. 2016; Cui et al. 2019a, b).

For check dams (i.e., with no slit), it was found that the analytical approach proposed by Jóhannesson et al. (2009) can capture the pileup height for granular materials well. This is because the compression of granular flow material, as well as the pileup mechanism characteristic of granular materials, is explicitly accounted for (Choi et al. 2015b). In contrast, the energy approach is more appropriate for water, for which there is little energy dissipation, and which primarily undergoes run-up since water has no shear strength, pileup cannot occur.

It is noted that both energy and momentum approaches (Jóhannesson et al. 2009 Armanini et al. 2011 Kwan 2012) were derived assuming that the barrier is closed (i.e., without any openings) so that no flow material can discharge. However, for the case of a slit dam, flow-structure interaction is more complicated. Run-up of flows against slit dams is a complex process that involves a combination of flow deceleration, redirection, and downstream discharge (Piton and Recking 2015a, b). Unlike check dams, slit dams usually have one or more slits to (i) reduce the flow peak discharge (compared to open channel flow) and (ii) to dissipate kinetic energy (Choi et al. 2016). The model proposed by Armanini et al. (2001) is able to predict the deposition height of granular materials deposited by a continuously flowing stream that passes a slit dam:

$$\frac{h_f}{h_i} = \frac{3}{2}\left(N_{Fr}\frac{w}{b}\right)^{\frac{2}{3}} - \frac{N_{Fr}^2}{2}\left\{1 - \left[1 - \frac{2}{3}\left(N_{Fr}\frac{w}{b}\right)^{-\frac{2}{3}}\right]^2\right\} \tag{3}$$

where w is the channel width and b is the slit size. However, this approach is only validated for flows with a solid fraction of up to 0.01 (Choi et al. 2016), which is substantially lower than the typical

Published online: 31 October 2019

solid fraction for granular debris flows, around 0.6 (Denlinger and Iverson 2001).

In this study, an analytical model based on the momentum approach was derived to predict the run-up heights of granular debris flows against slit dams. Furthermore, the interaction between granular debris flows and slit dams was studied numerically using the discrete element method (DEM) (Cundall and Strack 1979; Teufelsbauer et al. 2009). Investigations of granular debris flows with varying Froude conditions (N_{Fr}) impacting slit dams with different relative post spacings (b/d) were carried out. Run-up heights determined using the analytical models were compared with the numerical and reported experimental results. The influence of flow regime and the relative post spacing on the run-up height of granular debris flow was investigated.

Analytical model

To predict the run-up heights of granular debris flows against slit dams, a depth-averaged continuum model derived from assumptions similar to that of the momentum approach (Hákonardóttir 2003 Jóhannesson et al. 2009 Iverson et al. 2016) has been developed here. This analytical model is based on shock theory (Gray et al. 2003 Hákonardóttir 2003 Jóhannesson et al. 2009 Faug 2015; Faug et al. 2015 Iverson et al. 2016 Albaba et al. 2018). It assumes that the flow impinging on an obstacle is a one-dimensional dynamic problem which can be interpreted by the development of a shock. In this process, a shock (or shock wave), at which there are sudden jumps in the velocity, density, and height, develops immediately and travels upstream when a steady flow encounters a vertical obstacle. The incoming flow is assumed to be continuous, steady, uniform, compressible, and insensitive to the backwater effect, and the flow channel is horizontal (cf. Iverson et al. 2016; Savage et al. 1979).

Figure 1a shows a simplified sketch of a shock for granular debris flow against a check dam (a side view and a plan view). A shock develops and travels upstream with depth-invariant velocity u, height h, and bulk density ρ, while a granular dead zone forms between the shock and the dam. The conservation of mass and momentum across the shock travelling at speed s can be expressed as follows (cf. Jóhannesson et al. 2009 Iverson et al. 2016):

$$\rho_o h_o (u_o + s) = \rho_1 h_1 (u_1 + s) \tag{4}$$

$$\rho_o h_o u_o (u_o + s) + \int_o^{h_o} \sigma_{oxx}\, dz = \rho_1 h_1 u_1 (u_1 + s) + \int_o^{h_1} \sigma_{1xx}\, dz \tag{5}$$

where subscript o denotes properties of the flow upstream of the shock, subscript 1 denotes properties of the flow downstream from the shock, and σ_{xx} denotes the longitudinal normal stress.

As for the case of a slit dam (Fig. 1b), a more complex process is involved which includes a combination of flow deceleration, redirection, and downstream discharge. A shock develops and travels upstream at speed s as the incoming flow encounters the slit dam. Due to regulation of the slit dam, different from the check dam case, downstream flow from the shock transforms into two types: (i) one retards and deposits with speed u_1, forming a granular dead zone between the shock and the dam, which is similar to the check dam case, (ii) another propagates downstream with speed u_2 and then passes through the slit. The conservation of mass and momentum across the shock travelling at speed s can be expressed as follows:

$$\rho_o h_o (u_o + s) = (1-B)[\rho_1 h_1 (u_1 + s)] + B[\rho_2 h_2 (u_2 + s)] \tag{6}$$

$$\rho_o h_o u_o (u_o + s) + \int_o^{h_o} \sigma_{oxx}\, dz = (1-B)\left[\rho_1 h_1 u_1 (u_1 + s) + \int_o^{h_1} \sigma_{1xx}\, dz\right] + B\left[\rho_2 h_2 u_2 (u_2 + s) + \int_o^{h_2} \sigma_{1xx}\, dz\right] \tag{7}$$

where subscript o denotes properties of the flow upstream of the shock, subscript 1 denotes properties of the (i) retarding flow downstream of the shock while 2 denotes properties of the (ii) outgoing flow downstream of the shock. B ($B = b/w$, where b is the width of spacing between posts and w is the width of channel) is the transverse blockage of the slit dam. σ_{xx} is the longitudinal normal stress. Using of an assumption routinely employed in soil mechanics (Lambe and Whitman 1979), σ_{xx} can be expressed as follows:

$$\sigma_{xx} = k\sigma_{zz} = k\rho g(h - z) \tag{8}$$

where k is the longitudinal pressure coefficient, which denotes the ratio of longitudinal to vertical normal stress σ_{zz}. The k values of typical frictional debris roughly range from 0.2 to 5, depending on whether deformation occurs in an extensional or compressional mode (Iverson and Denlinger 2001). It was found that in the momentum approach, the assumption $k = 1$ yields good predictions of run-up heights of debris flows and it can even be used in more sophisticated run-up models (Iverson et al. 2016).

Considerable simplifications of Eqs. (6) and (7) can be obtained by introducing a reasonable assumption that the two types of flows downstream from the shock have the same density and height such that ρ_1 and h_1 are equal to ρ_2 and h_2, respectively. In this case, the mass jump condition (6) reduces to

$$s = \frac{\rho_o h_o u_o + B\rho_1 h_1 (u_1 - u_2) - \rho_1 h_1 u_1}{\rho_1 h_1 - \rho_o h_o} \tag{9}$$

Substitution of Eq. (8) in Eq. (7), and subsequent evaluation of the integrals for the momentum jump condition (7) yields

$$\rho_o h_o u_o (u_o + s) - B[\rho_1 h_1 u_2 (u_2 + s)] - (1-B)[\rho_1 h_1 u_1 (u_1 + s)] - \frac{1}{2} kg(\rho_1 h_1^2 - \rho_o h_o^2) = 0 \tag{10}$$

Downstream flow from the shock, the retarding flow deposits with speed u_1, forming a granular dead zone between the shock then the velocity u_1 can be supposed to be equal to 0. For the outgoing flow, the flow rheology between the shock and the slit dam is very complex with strong flow curvatures, flow redirection, and formation of dead zones in the corners. In want of a detailed theory for this region, we propose to consider an empirical linear relation between the outgoing velocity u_2 and the velocity u_o of the incoming flow:

$$u_2 = \alpha u_o \tag{11}$$

By combination of Eqs. (9) and (11), momentum jump condition (10) reduces to

$$Fr_o^2 [1 - 2B\alpha + B\alpha^2 - AB\alpha^2 + AB^2\alpha^2] - \frac{1}{2} k \left[A\frac{h_1}{h_o} - \frac{h_1}{h_o} - 1 + A^{-1}\right] = 0 \tag{12}$$

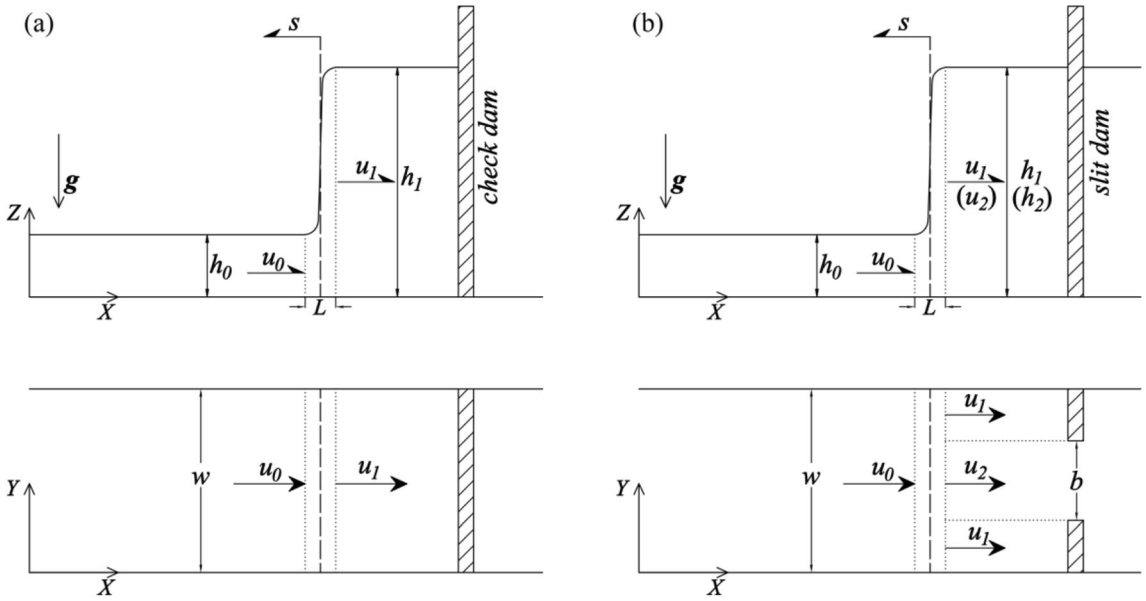

Fig. 1 Schematic drawing (side view and plan view) of run-up against **a** a check dam and **b** a slit dam

where $\mathrm{Fr}_o = u_o/\sqrt{gh_o}$, indicates the bulk characteristics of the incoming flow. The term A, which indicates the jump in density and height between the flows upstream and downstream of the shock, can be defined as follows:

$$A = \frac{\rho_1 h_1}{\rho_o h_o} \tag{13}$$

Equation (12) yields a run-up formula based on momentum approach, and it takes not only the upstream Froude conditions (N_{Fr}) but also the slit size (B) into consideration. For physically relevant parameter values ($\rho_1/\rho_o \sim 1$), Eq. (12) has three real roots, but only one of these roots has physical relevance by virtue of being positive and satisfying the jump condition requirement that $h_1 > h_o$ (cf. Iverson et al. 2016).

Considering two extreme cases that the dam is completely closed ($B = 0$) or open ($B = 1$), the boundary conditions of (12) can be expressed as

$$\begin{aligned} &\text{if } B = 0, \quad u_2 = 0 \rightarrow \alpha = 0 \\ &\text{if } B = 1, \quad u_2 = u_o \rightarrow \alpha = 1 \end{aligned} \tag{14}$$

Based on the boundary condition, α can be assumed as a function of B:

$$\alpha = f(B) \tag{15}$$

An explicit expression of Eq. (14) can be obtained by introducing an exponential form which can meet the boundary conditions in Eq. (13)

$$\alpha = B^e \tag{16}$$

where e is an empirical coefficient.

Finally, substituting Eq. (15) into (12), the solutions of the run-up formula can be obtained. Therefore, the run-up height of granular debris flows against slit dams can be predicted if the Froude number of the incoming flows and the geometry of the slit dams are known a priori.

Numerical model setup

The 3-D particulate flow code EDEM (DS Ltd 2004) is adopted to simulate the dynamics of granular flow in this study. In the DEM, contact forces and displacements of a stressed assembly of particles are found by tracing the movement of individual particles (Choi et al. 2014b). Compared to physical model tests, numerical simulations have a better capacity for capturing particle movements and interactions with structures (Zhou and Sun 2013; Chen et al. 2019).

Slit dams are usually comprised of a series of equally spaced rigid posts (Marchelli et al. 2019 Zhou et al. 2019). The spacing and the number of posts can be varied depending on the engineering design adopted. In this study, the interaction between granular debris flows and slit dams is studied by choosing a section which spans two adjacent posts since the processes which occur in the rest of the sections do not vary significantly with time. Figure 2 shows the numerical model setup. The channel inclination θ is fixed at 20° and gravitational acceleration g (9.81 m/s^2) acts downwards, along the vertical direction. Planar rigid geometry is constructed to model the channel bed and the slit dam. The sidewalls adopt periodic boundary conditions (PBC) (Rapaport and Rapaport 2004) which are applied along the flow direction and span the width of the channel (0.2 m). The PBC is required to eliminate the unrealistic particle arrangement at the wall boundary caused by the constraint of particle sizes in discrete element simulations (Rapaport and Rapaport 2004). A slit dam with rigid barriers and an adjustable spacing b is positioned downstream of the flows. The rigid barriers are set to be 2 m in height, perpendicular to the base of the channel. This is high enough to avoid potential overflow, so that the maximum run-up height can be captured, as per the assumptions in the equation derived.

Input parameters

The granular flows were composed of an assembly of 30,000 rigid spherical particles with a uniform diameter of 0.01 m. According to the commonly used values in numerical simulations of granular medium, the material density of each particle is 2630 kg/m^3 and the material shear modulus was set to be 24,000 MPa (Law et al. 2015; Ng et al. 2013). The contact friction angle of discrete elements was set as 31.5°, and the coefficient of restitution was set at 0.5 (cf. Song 2016; Chau et al. 2002). The interface friction angle was set as 16.6° which is consistent with the value determined by Choi et al. (2016) in laboratory tests. Details of the input parameters are given in Table 1.

Numerical testing procedures

The numerical study is divided into two stages: a preparation stage and an impact stage. In the preparation stage, all the particles fall freely and deposit randomly under boundary restrictions then a granular flow body with a continuous depth h of 0.05 m is prepared right behind the slit dam. Initial velocities u ranging from 0.38 to 5.7 m/s are uniformly applied to the assembly of particles. Calculating the Froude number by $N_{Fr} = u/\sqrt{gh\cos\theta}$, incoming granular flows with Froude numbers ranging from 0.5 to 7.5 are produced. The range of Froude number is consistent with that of reported channelized debris flows, which ranges from 0.5 to 7.6 based on field observations (Hübl et al. 2009 Scheidl et al. 2013 Cui et al. 2015).

In the impact stage, all the sidewall boundary restrictions are removed so the granular flows start to move and impact the slit dams. The relative post spacings ($R = b/d$) of slit dams range from 2 to 12, with the transverse blockage (B) between 10 and 60% (Silva et al. 2016; Choi et al. 2016). A control test without spacing was also conducted for reference. A summary of the numerical test plans is given in Table 2.

Model calibration

To ensure that the input parameters and modelling methodology are able to simulate the interaction between granular flows and slit dams, numerical simulation of the granular flows was compared with experimental results reported by Choi et al. (2016). Figure 3 shows a comparison of flow kinematics between experimental tests and numerical simulations: the granular flow behaviors of flume tests are shown on the left (Fig. 3(a1–a3)) while the pertinent numerical results by DEM are shown on the right (Fig. 3(b1–b3)). A wedge-shaped flow front (Choi et al. 2014a) with a Froude number of 2.3 arrives behind the barrier at t = 0.2 s (Fig. 3(a1, b1)); subsequently, particles in the flow front run-up along the rigid barrier like water at t = 0.4 s (Fig. 3(a2, b2)); subsequent granular flow impacts and piles up on top of the existing deposits, forming a ramp-like dead zone (Gray et al. 2003) at t = 0.6 s (Fig. 3(a3, b3)). Thereafter, the dead zone continues to thicken and expand upstream until the arrest of granular motion for all particles.

It is observed that the flow kinematics from flume experiments and the calibrated model are consistent. The agreements of the Froude number and flow kinematics between the numerical and experimental results indicate that the set of input parameters and the numerical model used for this study can effectively model the interaction between granular debris flows and slit dams, and the basic mechanisms can be captured.

Interpretation of DEM results

Granular flow run-up mechanism

Figure 4 shows a side view of the impact and run-up process of a subcritical flow (N_{Fr} = 0.5) and a supercritical flow (N_{Fr} = 6.5), respectively. At t = 0 s, both subcritical and supercritical flows approach the barrier with an identical flow height (Fig. 4(a1, b1)). For the subcritical flow, a typical pileup mechanism can be observed: the granular bore continues to thicken while the run-up height does not change (Choi et al. 2015b). At t = 0.1 s, the granular flow impacts the slit dam and most particles in front of the flow deposit behind the rigid barrier, forming a ramp-like dead zone at the base of the barrier while a small number of particles pass through the slit between the posts (Fig. 4(a2)). As subsequent flow material impacts the existing deposits, the pileup continues to develop, and the dead zone expands upward (Fig. 4(a3)). Thereafter, the dead zone continues to thicken while maintaining a constant height (Fig. 4(a4, a5)). Numerical simulation results indicate that subcritical granular flows exhibit distinct pileup characteristics which are consistent with the experimental observation of Armanini et al. (2011) and Choi et al. (2015b).

Supercritical granular debris flows resulted to a combination of a vertical jet run-up and a pileup mechanism. At t = 0 s, a distinct upward jet along the barrier forms as the supercritical flow impacts the slit dam (Fig. 4(b2)). Such a run-up mechanism is more reminiscent of the vertical jet mechanism described by Armanini et al. (2011) and Choi et al. (2015b) for liquid flows and is consistent with Ng et al. (2017) and Cui et al. (2018) for granular flows of large glass particles. Subsequently, run-up continues to develop and the run-up height keeps increasing. Simultaneously, a large number of particles pass through the spacing, discharging dispersedly as a downstream jet. (Fig. 4(b3)). When the maximum run-up height is reached, the run-up process ceases. Concurrently, the pileup process begins: the dead zone keeps thickening while its height remains unchanged (Fig. 4(b4)). The numerical simulation results demonstrate that the run-up mechanism between subcritical and supercritical granular flows are quite different, subcritical granular flows only exhibit a pileup mechanism while supercritical flows show a combination of vertical jet run-up and pileup mechanism.

Figure 5 shows the evolution of run-up heights. In this numerical study, the initial incoming flow is homogeneous, steady, and uniform so that the run-up height grows without intense fluctuation. Figure 5a shows the time series of run-up heights in simulations of different Froude numbers. For the flows with low Froude numbers (e.g., $N_{Fr} < 3.5$), the run-up height rapidly reaches its peak values and then maintains an almost constant level. For flows with high Froude numbers (e.g., $N_{Fr} > 4.5$), the run-up height keeps increasing until the maximum run-up height is reached. This increase is non-linear: the growth rate varies in different periods. At first, the run-up heights rapidly increase and the growth rate reaches its peak value as the flow front impacts the dam. Thereafter, the growth rate decreases over time, while the run-up process gradually ceases. After reaching the peak value, the run-up heights decrease slowly and then maintain a constant level, indicating that the pileup process is underway. Figure 5b shows the time series of run-up heights for different relative post spacings. Numerical simulation results reveal that the evolution of run-up heights in different relative post spacings shares a similar tendency: the run-up height increases over time to a peak value then remains at a

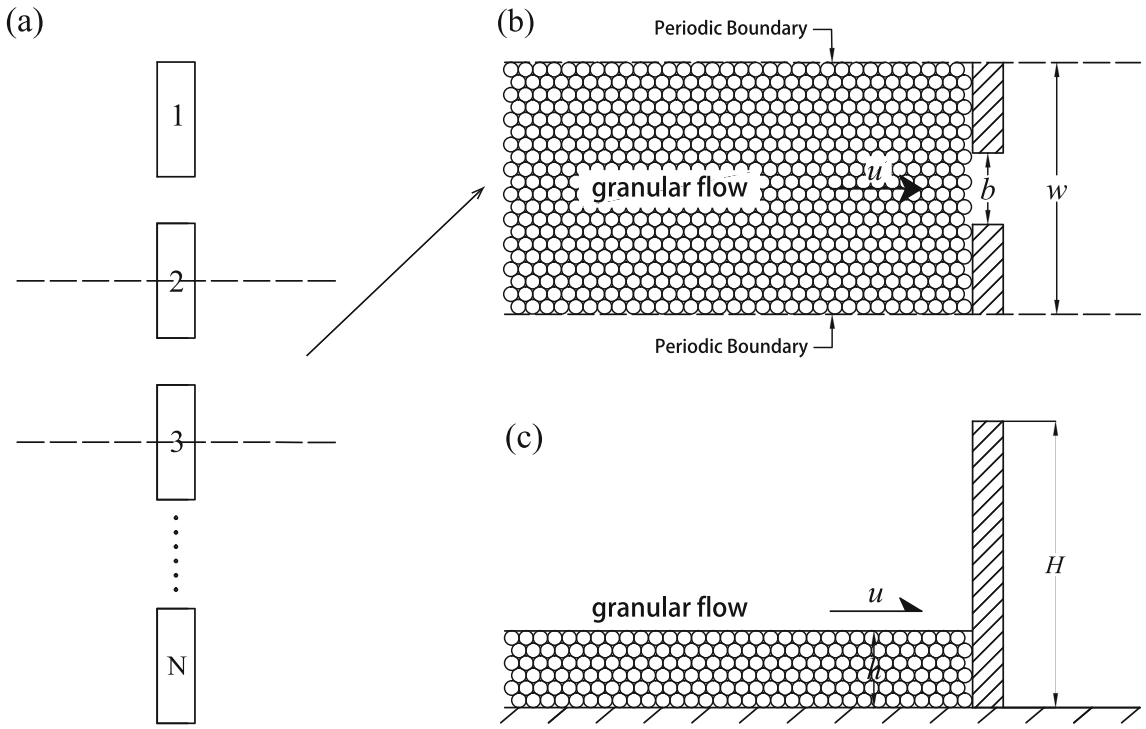

Fig. 2 Numerical model. **a** A chosen section of slit dam. **b** Plan view of the chosen section. **c** Side view of the chosen section

constant level. The run-up height evidently depends on relative post spacing: the greater the relative post spacing, the lower the maximum run-up height and the lesser time it takes to reach it. These results indicate that the slit size affects the run-up of granular flows against slit dams (see later sections).

Comparison of run-up prediction models

Figure 6 shows the relationship between the transverse blockage B and the normalized outflow velocity $\alpha = u_2/u_o$. The numerical simulation results show that as the transverse blockage B of slit dams increases, the normalized outflow velocity increases monotonically. Granular debris flows with different Froude conditions (N_{Fr}) all meet with this tendency. This trend is consistent with the assumption we have made in our analytical model (see "Analytical model" section). By plotting B against α, it is found that the best match can be obtained when the empirical coefficient e is equal to 1.519.

Table 1 DEM input parameters

Input parameter	Value
Number of discrete elements	50000
Particle diameter (m)	0.01
Density (kg/m^3)	2630
Total mass of particles (kg)	68.85
Shear modulus (MPa)	24,000
Discrete element/wall friction	0.3
Discrete element friction	0.6
Rolling friction coefficient	0.01
Coefficient of restitution	0.5

Figure 7a shows the comparison between the simulated normalized run-up heights and the analytical approach of Armanini and Larcher (2001). The results illustrate that this approach cannot predict the run-up heights of granular flows well: the predictions are too high when the relative post spacing is low but are too conservative when the relative post spacing is high. This is because this approach assumes that run-up process is under the hydraulic jump condition (Armanini and Larcher 2001), making it inappropriate for frictional dense granular flows, in which the flow-structure interaction mechanism is dominated by pileup (Choi et al. 2016).

It is reported that the momentum approach can capture the run-up mechanism of granular flows and can predict the run-up heights well (Choi et al. 2015b Iverson et al. 2016 Ng et al. 2017). Using the analytical model derived here (see "Analytical model"), Fig. 7b shows a comparison between the simulated normalized run-up heights and the modified momentum approach in this study. The results indicate that this model can indeed predict the run-up heights of the granular debris flows against slit dams quite well. Run-up heights predicted by this model show the same tendency with the numerical simulation results: higher Froude number (N_{Fr}) and lower transverse blockage (B) lead to higher run-up heights. The maximum error between the predicted run-up heights and the numerical results is below 15.6%. According to these results, engineers anticipating a dense granular debris flow can safely use the newly derived equation to estimate the height required for the slit dam to avoid dangerous overtopping. Furthermore, the results show the influence of the upstream Froude conditions (N_{Fr}) on run-up heights for granular flows against slit

Table 2 Numerical simulation plan

Relative post spacing ($R = b/d$)	Transverse blockage ($B = b/w$) (%)	Initial Froude condition (N_{Fr})
0	0	0.5; 1.5; 2.5; 3.5; 4.5; 5.5; 6.5; 7.5
2	10	
4	20	
6	30	
8	40	
10	50	
12	60	

dams. As the Froude number of an incoming flow increases, the maximum run-up height increases monotonically, which is consistent with Choi et al. (2015b), Iverson et al. (2016), and Ng et al. (2017).

Figure 8 shows a comparison of the normalized run-up height predicted by Armanini and Larcher (2001) and the momentum approach with the reported experimental results (Choi et al. 2016). It is noted that experimental results match well with the run-up heights predicted by the momentum approach proposed in this study while the analytical approach of Armanini and Larcher (2001) tends to overestimate, consistent with the DEM numerical result comparisons.

The granular debris flow is composed of an assembly of numerous discrete particles. Therefore, the particle-particle interactions and particle-barrier interactions do significantly affect the flow dynamics and then pose a strong influence on the run-up behavior. However, all the analytical prediction models based on continuum hypothesis (Hákonardóttir 2003 Jóhannesson et al. 2009 Armanini et al. 2011 Kwan 2012) fail to consider the particle-particle interactions, which should be taken into consideration in run-up height prediction.

Influence of the relative post spacing on run-up height

Jamming occurs when the flow of grains through a spacing and the size of the outlet is not large enough (Janda et al. 2008). Such a jamming is the response of a system to the applied external

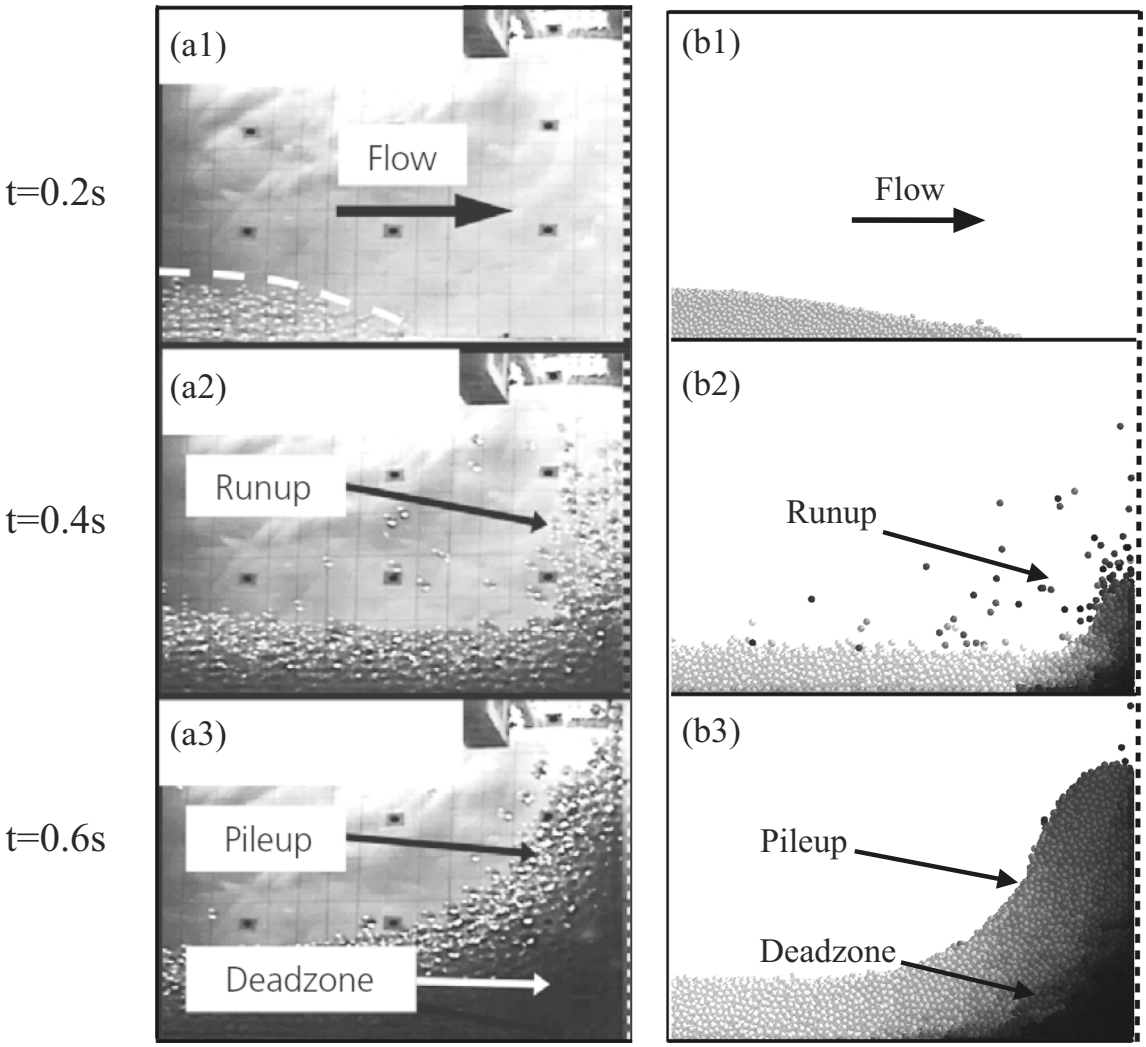

Fig. 3 Comparison of flume experiments and computed flow kinematics (test C30-D1-SD5, wherein inclination = 30°, b/d = 5.0). The color of particles denotes the velocity of particles, and the darker the color, the lower the velocity

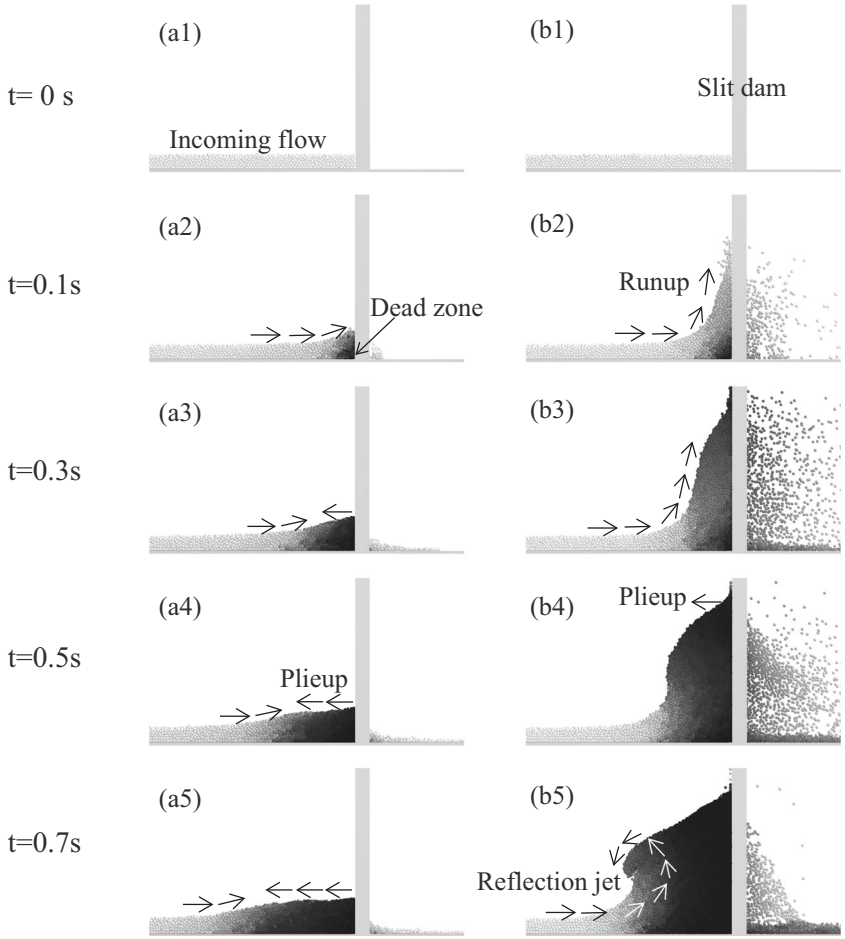

Fig. 4 Simulated flow kinematics for subcritical flow (N_{Fr} = 0.5) (a1–a5) and supercritical flow (N_{Fr} = 6.5) (b1–b5), b/d = 2.0. The color of particles denotes the velocity of particles, and the darker the color, the lower the velocity

stresses by developing mechanical structures that block the flow. In granular materials, these structures are called "arches" (Zuriguel et al. 2005). For the case of granular debris flows impacting slit dams, flow material can jam behind the dam due to the formation of arches when the post spacing is not large enough (Law et al. 2015). Figure 9a shows a typical formation of arches of granular flow behind a slit dam. As the flow front impacts the slit dam, granular material is subjected to a reflective dynamic impact force from the barrier. Driven by the applied stress, particles in front of the flow rearrange and the structure of the force chains changes, forming an arch (Terzaghi 1943). Due to the formation of arches, subsequent granular flow tends to slow down or halt (Arévalo and Zuriguel 2016).

Figure 9b shows the evolution of the granular outflow rate for slit dams with different relative post spacings. It can be seen that outflow rate increases with the relative post spacing since the wider the spacing, the more flow material can pass through. It was found that the evolution of the outflow rate tends to fluctuate periodically, which may be related to the formation of arches. When arches form, granular material blocks the opening and momentarily halts subsequent flow, which leads to a decrease in outflow rate: from a local maximum value to minimum. On the other hand, the outflow rates tend to increase from a local minimum value to the maximum if the arches collapse. It was also found that the formation of arches is influenced by the slit size. Arches are formed easier at low relative post spacings, at times resulting to near zero outflow rates. As the relative post spacing increases, there are lesser instances at which arches form and the outflow rate can easily reach its minimum level.

In analytical models, the maximum normalized run-up height decreases monotonically as the transverse blockage increases (Armanini and Larcher 2001). Such a principle is validated for granular flow problems with a maximum solid volume fraction of 0.01 (Choi et al. 2016). However, for frictional flows such as granular flows, the formation of arches and the interparticle contact should be taken into consideration. When the relative post spacing is small, particles in front of the flow can jam easily behind the slit dam, blocking the subsequent flow and resulting to a maximum run-up height that is usually larger than expected.

Figure 10 shows the relationship between the normalized maximum run-up heights and relative post spacings. The numerical simulation results are compared with experimental data (Choi et al. 2016), which has a similar configuration in channel geometry,

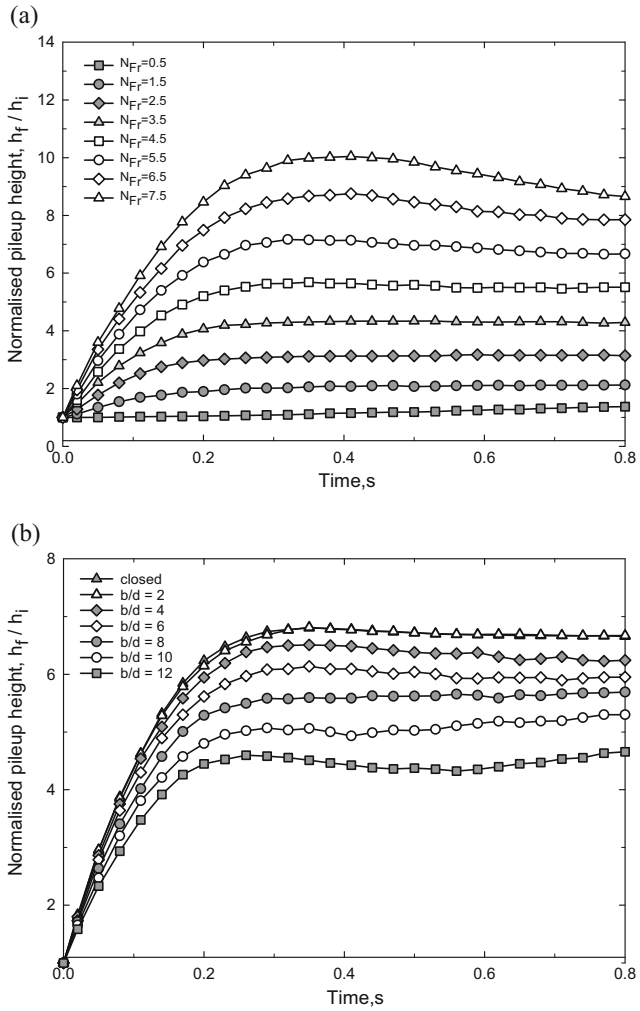

Fig. 5 Evolution of the run-up height. **a** $b/d = 4.0$. **b** $N_{Fr} = 4.5$, where zero time corresponds to the time instance at which the flow front reaches the dam

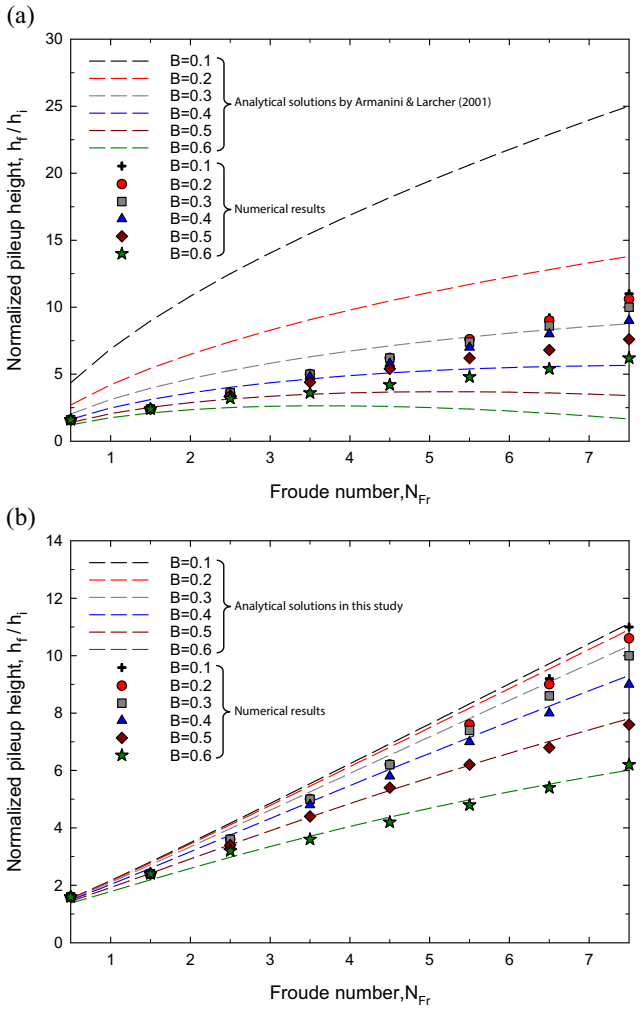

Fig. 7 Comparison of theoretical normalised run-up height predicted by **a** the energy approach and **b** the momentum approach ($e = 1.519$) with the DEM results

granular material property and slit structure type with study while Froude numbers are smaller than 2.3.

For low Froude numbers ($N_{Fr} \leq 2.5$), the run-up heights of the numerical study are very close to the measured values by Choi et al. (2016). The results show that the normalized maximum run-up height is not strongly influenced by the relative post spacing.

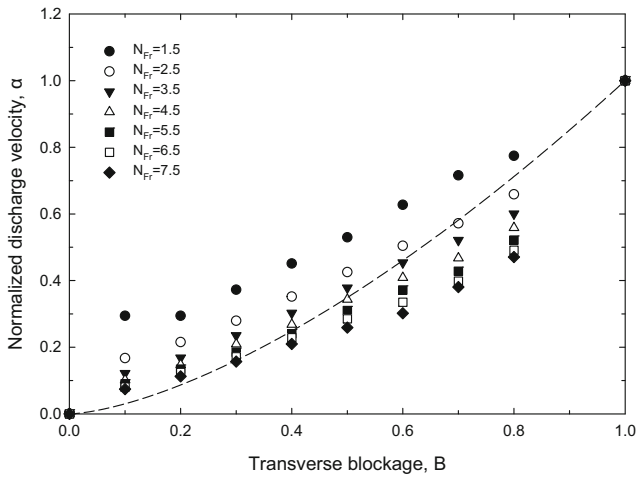

Fig. 6 Relationship between transverse blockage and normalized outflow velocity

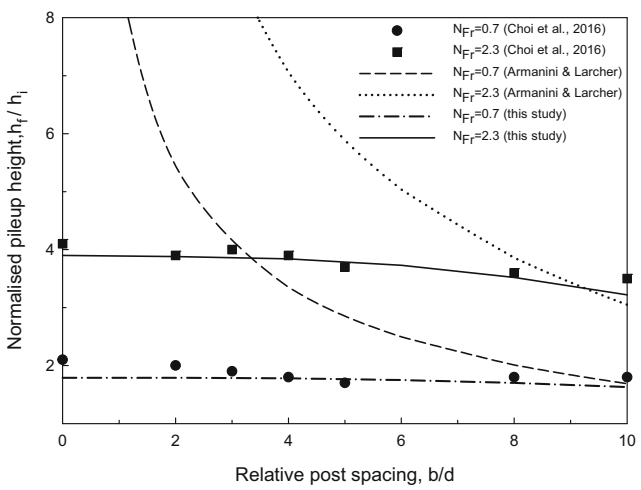

Fig. 8 Comparison of theoretical normalised run-up height predicted by the energy approach and the momentum approach ($e = 1.519$) with the reported experimental results

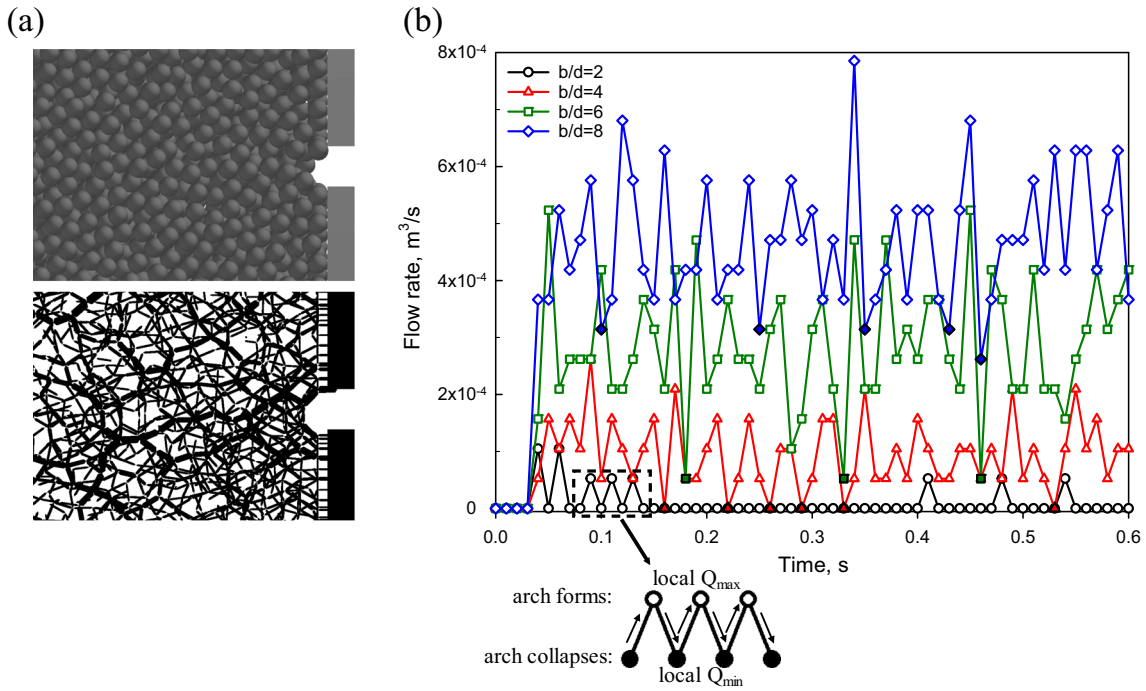

Fig. 9 **a** Arches and force chains in granular flow behind a slit dam ($N_{Fr} = 0.5$; $b/d = 2.0$). **b** Evolution of the granular outflow rate for slit dams with different relative post spacing b/d (solid point denotes the local Q_{min})

This is because stable arches can easily form at the slit, provided that the Froude number of the incoming flow is low ($N_{Fr} \leq 2.5$). In this case, there is no significant difference between slit dams of different slit sizes since the stable arches can block the outlet and halt the flows. When the Froude number is high ($N_{Fr} \geq 2.5$), supercritical flows with high velocities can break arches easily (Choi et al. 2016). Pardo and Sáez (2014) observed that the arch strength evidently depends on the its length: shorter arches are generally stronger because higher contact stresses can be maintained during constrictions. The length of arches is directly related to the relative post spacing and the probability of formation of stable arches decreases as b/d increases (Janda et al. 2008 Arévalo and Zuriguel 2016 Marchelli et al. 2019). In this case, the relative post spacings affect the run-up height significantly. In general, the maximum run-up height declines as the ratio b/d increases. The results show that there is a critical value of relative post spacing (R_C): within the critical value, the maximum run-up height is insensitive (the decrease rate is within 5%) to the relative post spacing; once b/d exceeds the critical value, the maximum run-up height decreases rapidly as the relative post spacing increases. Such a critical value has been studied in many previous works, and it is noted that a fixed value for R_C does not exist (Zuriguel et al. 2005 Janda et al. 2008).

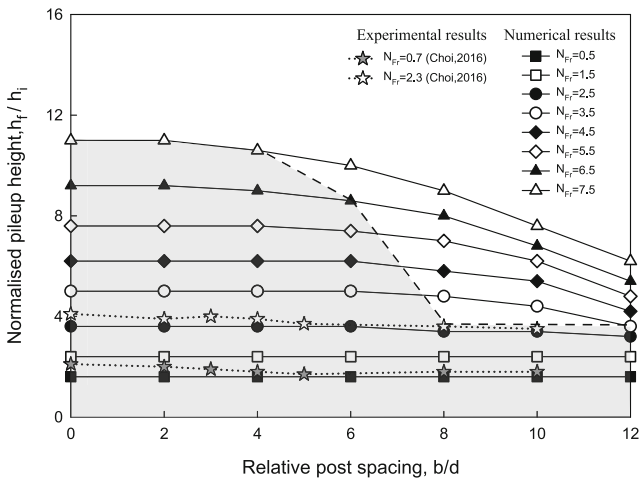

Fig. 10 Relationship between run-up height and relative post spacing

As shown in Fig. 10, the numerical results can be interpreted by demarcating two zones. In zone I ($b/d \leq R_C$, shadow area), the run-up heights maintain a constant level within a critical range of the relative post spacing. The critical value Rc decreases with the increase of N_{Fr} so that zone I shrinks as the Froude number of incoming flows increases. In zone II ($b/d \geq R_C$, light area), the relative post spacing has a significant effect on the run-up height: the maximum run-up height decreases rapidly as b/d increases. Zone II expands as N_{Fr} increases and eventually spans the full range of the relative post spacing when the Froude number of the flow is high enough. In this case, granular material fails to form stable arches and the run-up height decreases monotonically as the relative post spacing increases.

Conclusions

An analytical model based on the momentum approach was derived to predict the run-up heights of granular debris flows against slit dams. A numerical study of granular debris flows impacting slit dams by discrete element method (DEM) was conducted. The numerical results were compared with analytical models and reported experimental data. The influence of the Froude number (N_{Fr}) and relative post spacing (b/d) on the run-up height was investigated. The conclusions from this study can be drawn as follows:

(a) An analytical model based on the momentum approach which considers the effect of the flow regime and the post spacing size is proposed. This model can capture the run-up mechanism of granular debris flows against slit dams and predict the run-up heights quite well.
(b) The run-up mechanisms between subcritical and supercritical granular flows are different: subcritical granular flows result in a typical pileup mechanism, whereas supercritical flows lead to a combination of vertical jet run-up and pileup mechanism.
(c) When the Froude number of the incoming flow is low ($N_{Fr} \leq 2.5$), the run-up height is not strongly influenced by the relative post spacing. When the Froude number is high ($N_{Fr} > 2.5$), there is a critical value of relative post spacing (R_C): within the critical value, the maximum run-up height is insensitive to the relative post spacing; once b/d exceeds the critical value, the maximum run-up height decreases as the relative post spacing increases.

The series of numerical simulations by DEM is aimed at investigating the effect of the Froude number (N_{Fr}) and relative post spacing (b/d) on the run-up mechanism. By introducing a single-phase model, the effect of fluid in debris flows is not taken into consideration. In the further study, it is worth to explore on the interactions between solid-liquid two-phase debris flows and slit dams.

Funding information The authors received financial support from the National Natural Science Foundation of China (grant nos. 11672318, 51809261); the Key Research Program of Frontier Sciences, Chinese Academy of Sciences (CAS) (grant no. QYZDB-SSW-DQC010); and the 135 Strategic Program of the Institute of Mountain Hazards and Environment, CAS (grant no. SDS-135-1701) and the Research Grants Council of the Hong Kong Special Administrative Region, China (Project Nos. AoE/E-603/18; T22-603/15N; 16209717; 16212618)

References

Albaba A, Lambert S, Faug T (2018) Dry granular avalanche impact force on a rigid wall: analytic shock solution versus discrete element simulations. Phys Rev E 97(5):052903
Arévalo R, Zuriguel I (2016) Clogging of granular materials in silos: effect of gravity and outlet size. Soft Matter 12(1):123–130
Armanini A, Larcher M (2001) Rational criterion for designing spacing of slit-check dam. J Hydraul Eng 127(2):94–104
Armanini A, Larcher M, Odorizzi M (2011) Dynamic impact of a debris flow front against a vertical wall. In Proceedings of the 5th International Conference on Debris-Flow Hazards Mitigation: Mechanics, Prediction and Assessment, pp. 1041-1049 Padua, Italy
Chau K, Wong RHC, Wu JJ (2002) Coefficient of restitution and rotational motions of rockfall impacts. Int J Rock Mech Min Sci 39(1):69–77
Chen HX, Li J, Feng SJ, Gao HY, Zhang DM (2019) Simulation of interactions between debris flow and check dams on three-dimensional terrain. Eng Geol 251:48–62
Choi CE, Ng CWW, Song D, Kwan JHS, Shiu HYK, Ho KKS, Koo RCH (2014a) Flume investigation of landslide debris–resisting baffles. Can Geotech J 51(5):540–553
Choi CE, Ng CWW, Law RP, Song D, Kwan JSH, Ho KKS (2014b) Computational investigation of baffle configuration on impedance of channelized debris flow. Can Geotech J 52(2):182–197
Choi CE, Ng CWW, Au-Yeung SCH, Goodwin GR (2015a) Froude characteristics of both dense granular and water flows in flume modelling. Landslides 12(6):1197–1206
Choi CE, Au-Yeung SCH, Ng CWW, Song D (2015b) Flume investigation of landslide granular debris and water runup mechanisms. Géotechn Lett 5(1):28–32
Choi CE, Goodwin GR, Ng CWW, Cheung DKH, Kwan JS, Pun WK (2016) Coarse granular flow interaction with slit structures. Géotechn Lett 6(4):267–274
Chu T, Hill G, McClung DM, Ngun R, Sherkat R (1995) Experiments on granular flows to predict avalanche runup. Can Geotech J 32(2):285–295
Cui P, Zeng C, Lei Y (2015) Experimental analysis on the impact force of viscous debris flow. Earth Surf Process Landf 40(12):1644–1655
Cui Y, Choi CE, Liu LH, Ng CWW (2018) Effects of particle size of mono-disperse granular flows impacting a rigid barrier. Nat Hazards 91(3):1179–1201
Cui Y, Cheng D, Choi CE, Jin W, Lei Y, Kargel JS (2019a)The cost of rapid and haphazard urbanization: lessons learned from the Freetown landslide disaster. Landslides 16(6):1167–1176
Cui Y, Jiang Y, Guo C (2019b) Investigation of the initiation of shallow failure in widely graded loose soil slopes considering interstitial flow and surface runoff. Landslides 16(4):815–828
Cundall PA, Strack OD (1979) A discrete numerical model for granular assemblies. Geotechnique 29(1):47–65
DEM Solutions Ltd (2014) EDEM Version 2.6.0 User Guide. Edinburgh
Denlinger RP, Iverson RM (2001) Flow of variably fluidized granular masses across three-dimensional terrain: 2. Numerical predictions and experimental tests. J Geophys Res Solid Earth 106(B1):553–566
Faug T (2015) Depth-averaged analytic solutions for free-surface granular flows impacting rigid walls down inclines. Phys Rev E 92(6):062310
Faug T, Childs P, Wyburn E, Einav I (2015) Standing jumps in shallow granular flows down smooth inclines. Physics of Fluids 27:073304
Gray JMNT, Tai YC, Noelle S (2003) Shock waves, dead zones and particle-free regions in rapid granular free-surface flows. J Fluid Mech 491:161–181
Hákonardóttir KM (2003) A laboratory study of the interaction between supercritical, shallow flows and dams. Icelandic Meteorological Office (Vedurstofa Islands) Report 03038
Hübl J, Suda J, Proske D, Kaitna R, Scheidl C (2009) Debris flow impact estimation. In Proceedings of the 11th international symposium on water management and hydraulic engineering, Ohrid, Macedonia pp.1-5
Hungr O, McClung DM (1987) An equation for calculating snow avalanche runup against barriers. National Research Council Canada, Institute for Research in Construction, pp 602–622
Hungr O, Morgan GC, Kellerhals R (1984) Quantitative analysis of debris torrent hazards for design of remedial measures. Can Geotech J 21(4):663–677
Iverson RM (1997) The physics of debris flows. Rev Geophys 35(3):245–296
Iverson RM, Denlinger RP (2001) Flow of variably fluidized granular masses across three-dimensional terrain: 1. Coulomb mixture theory. J Geophys Res Solid Earth 106(B1):537–552
Iverson RM, George DL, Logan M (2016) Debris flow runup on vertical barriers and adverse slopes. J Geophys Res Earth Surf 121(12):2333–2357
Jakob M, Hungr O, Jakob DM (2005) Debris-flow hazards and related phenomena Vol. 739. Springer, Berlin
Janda A, Zuriguel I, Garcimartín A, Pugnaloni LA, Maza D (2008) Jamming and critical outlet size in the discharge of a two-dimensional silo. EPL (Europhys Lett) 84(4):44002
Jóhannesson T, Gauer P, Issler P, Lied K, Hákonardóttir KM (2009) The design of avalanche protection dams: recent practical and theoretical developments
Kwan JSH (2012) Supplementary technical guidance on design of rigid debris-resisting barriers. Geotechnical Engineering Office, HKSAR. GEO Report (270)
Lambe TW, Whitman RV (1979) Soil mechanics, SI version. Wiley, New York
Law RPH, Choi CE, Ng CWW (2015) Discrete-element investigation of influence of granular debris flow baffles on rigid barrier impact. Can Geotech J 53(1):179–185
Mancarella D, Hungr O (2010) Analysis of runup of granular avalanches against steep, adverse slopes and protective barriers. Can Geotech J 47(8):827–841
Marchelli M, Leonardi A, Pirulli M, Scavia C (2019) On the efficiency of slit-check dams in retaining granular flows. Géotechnique:1–39
Ng CWW, Choi CE, Law RP (2013) Longitudinal spreading of granular flow in trapezoidal channels. Geomorphology 194:84–93
Ng CWW, Song D, Choi CE, Liu LHD, Kwan JSH, Koo RCH, Pun WK (2016) Impact mechanisms of granular and viscous flows on rigid and flexible barriers. Can Geotech J 54(2):188–206
Ng CWW, Choi CE, Liu LHD, Wang Y, Song D, Yang N (2017) Influence of particle size on the mechanism of dry granular runup on a rigid barrier. Géotechn Lett 7(1):79–89

Pardo GS, Sáez E (2014) Experimental and numerical study of arching soil effect in coarse sand. Comput Geotech 57:75–84
Piton G, Recking A (2015a) Design of sediment traps with open check dams. I: hydraulic and deposition processes. J Hydraul Eng 142(2):04015045
Piton G, Recking A (2015b) Design of sediment traps with open check dams. II: woody debris. J Hydraul Eng 142(2):04015046
Rapaport DC, Rapaport DCR (2004) The art of molecular dynamics simulation. Cambridge University Press, pp 120–152
Savage SB (1979) Gravity flow of cohesionless granular materials in chutes and channels. Journal of Fluid Mechanics 92:53–96
Scheidl C, Chiari M, Kaitna R, Müllegger M, Krawtschuk A, Zimmermann T, Proske D (2013) Analysing debris-flow impact models, based on a small scale modelling approach. Surv Geophys 34(1):121–140
Shen W, Zhao T, Zhao J, Dai F, Zhou GG (2018) Quantifying the impact of dry debris flow against a rigid barrier by DEM analyses. Eng Geol 241:86–96
Silva M, Costa S, Canelas RB, Pinheiro AN, Cardoso AH (2016) Experimental and numerical study of slit-check dams. International Journal of Sustainable Development and Planning, 11(2):107–118
Song D (2016) Mechanisms of debris flow impact on rigid and flexible barriers (Doctoral dissertation)
Terzaghi K (1943) Arching in ideal soils. In Theoretical soil mechanics. Wiley, Hoboken
Teufelsbauer, H Wang, Y Chiou, MC, Wu W (2009) Flow–obstacle interaction in rapid granular avalanches: DEM simulation and comparison with experiment. Granular Matter 11(4):209–220
Watanabe M, Mizuyama T, Uehara S (1980) Review of debris flow countermeasure facilities. Journal of the Japan Erosion Control Engineering Society 115(115):40–45
Zhou GG, Sun QC (2013) Three-dimensional numerical study on flow regimes of dry granular flows by DEM. Powder Technol 239:115–127
Zhou GG, Hu HS, Song D, Zhao T, Chen XQ (2019) Experimental study on the regulation function of slit dam against debris flows. Landslides:1–16
Zuriguel I, Garcimartín A, Maza D, Pugnaloni LA, Pastor JM (2005) Jamming during the discharge of granular matter from a silo. Phys Rev E 71(5):051303

G. G. D. Zhou · J. Du (✉) · D. Song · H. S. Hu
Key Laboratory of Mountain Hazards and Earth Surface Process/Institute of Mountain Hazards and Environment,
Chinese Academy of Sciences (CAS),
Chengdu, China
Email: dujunhan17@mails.ucas.ac.cn

G. G. D. Zhou
e-mail: gordon@imde.ac.cn

D. Song
e-mail: drsong@imde.ac.cn

H. S. Hu
e-mail: huhongsen15@mails.ucas.edu.cn

G. G. D. Zhou · J. Du · D. Song · H. S. Hu
University of Chinese Academy of Sciences,
Beijing, China

C. E. Choi
Department of Civil Engineering,
The University of Hong Kong,
Pok Fu Lam, Hong Kong
e-mail: cechoi@hku.hk

C. Jiang
Kunming Dongchuan Debris Flow Prevention and Control Institute,
Kunming, China
e-mail: 282955245@qq.com